J Korean Soc Appl Biol Chem (2015) 58(6):877–885
DOI 10.1007/s13765-015-0116-9

Online ISSN 2234-344X
Print ISSN 1738-2203

ARTICLE

ToxB encodes a canonical GTP cyclohydrolase II in toxoflavin biosynthesis and *ribA* expression restored toxoflavin production in a Δ*toxB* mutant

Minae Joo[1] · Hye-Gyeong Yoo[1] · Hyun-Ju Kim[1] · Hyung-Jin Kwon[1]

Received: 11 July 2015 / Accepted: 22 August 2015 / Published online: 7 September 2015

Abstract *Burkholderia glumae* synthesizes toxoflavin, a phytotoxin that contributes the virulence of this phytopathogen. The toxoflavin biosynthetic gene cluster contains a *tox* operon composed of five genes, *toxABCDE*, and *toxB* is predicted to encode a GTP cyclohydrolase II, which is the first enzyme (RibA) in riboflavin biosynthesis. ToxE is also homologous to RibD, the bifunctional deaminase/reductase acting on the RibA product. This suggests that toxoflavin and riboflavin biosynthesis share the first two steps in their respective biosyntheses. In this study, we demonstrated that ToxB and *B. glumae* RibA (Bglu-RibA) both displayed GTP cyclohydrolase II activity with comparable kinetic parameters. When *toxB* was inactivated, toxoflavin production was abolished, and introduction of a plasmid copy of *Bglu-ribA* restored toxoflavin production in a Δ*toxB* mutant. ToxB and Bglu-RibA can thus be defined as GTP cyclohydrolase II isozymes, even though *Bglu-ribA* is not a genetic equivalent of *toxB* because the chromosomal copy of *Bglu-ribA* is unable to support toxoflavin production in the absence of *toxB*. In LB agar culture, *toxAB* is incapable of complementing Δ*toxB* though *toxABC* induced toxoflavin accumulation in the Δ*toxB* mutant up to 80 % of the WT level. This indicates that *toxBC* co-expression is a critical factor for toxoflavin biosynthesis in this condition, suggesting that the WD repeat protein ToxC acts as a scaffolding protein in a toxoflavin biosynthetic metabolon. In LB liquid culture, *toxAB* successfully restored toxoflavin production, suggesting that a role of *toxBC* co-expression is dependent upon growth condition.

✉ Hyung-Jin Kwon
hjink@mju.ac.kr

[1] Division of Bioscience and Bioinformatics, Myongji University, Yongin 449-728, Republic of Korea

Keywords *Burkholderia glumae* · GTP cyclohydrolase II · *ribA* · *toxB* · Toxoflavin

Introduction

Toxoflavin, fervenulin, and reumycin are 7-azapteridine antibiotics with bacterial origins (Machlowitz et al. 1954). Toxoflavin was later identified as a key player in the virulence of *Burkholderia glumae*, a rice pathogen (Sato et al. 1989; Yoneyama et al. 1998; Kim et al. 2004). An early biosynthetic study on toxoflavin in *Pseudomonas cocovenenans* substantiated its origin of a purine derivative (Levenberg and Kaczmarek 1966; Levenberg and Linton 1966). Together with these results, the knowledge of riboflavin biosynthesis (Fischer and Bacher 2005; Gräwert et al. 2013) guides us to deduce the involvement of GTP cyclohydrolase II and deaminase/reductase activities in toxoflavin biosynthesis (Fig. 1A). GTP cyclohydrolase II (RibA) that mediates a committed step in riboflavin biosynthesis converts GTP into an anomeric pair of **1**, involving a guanine ring opening and release of formate and pyrophosphate (Ritz et al. 2001). Structural and mechanistic analysis of RibA revealed a catalytic arginine residue that is involved in the generation of a covalent guanylyl-RibA intermediate with pyrophosphate release (Ren et al. 2005). This enzyme-bound intermediate undergoes an imidazole ring-opening event and formate is subsequently released (Ritz et al. 2001; Schramek et al. 2001). The resulting product of **1** was then hydrolyzed from RibA. Kinetics study of RibA reaction indicated that the first chemical event of the reactions is the rate-determining step, suggesting that a slow formation of guanylyl-RibA intermediate controls the overall turnover number of RibA (Schramek et al. 2001); pre-steady state quenched

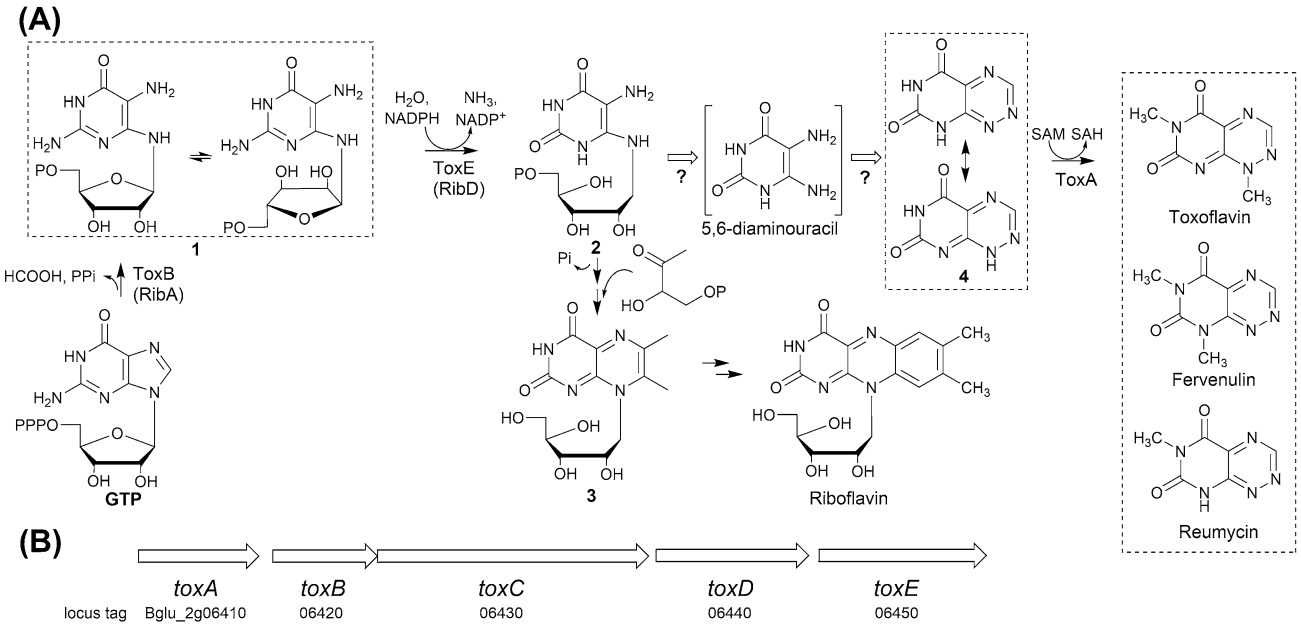

Fig. 1 Toxoflavin biosynthetic pathway. (**A**) The proposed toxoflavin biosynthetic pathway with comparisons to that of riboflavin. (**B**) Genetic organization of *tox* operon

flow analysis of RibA demonstrated that GTP was consumed at a rate constant of 0.064/s and the final product was formed at an apparent rate constant of 0.062/s.

Transposon mutagenesis and subsequent targeted gene inactivation studies identified the toxoflavin biosynthesis locus (*toxABCDE*) from *B. glumae* and the presence of *toxB*, a gene homologous to that of GTP cyclohydrolase II asserted the GTP origin of toxoflavin (Kim et al. 2004; Suzuki et al. 2004) (Fig. 1B). The *ribA* candidate (bglu_2g14580) of *B. glumae* bears a modest homology to *toxB* (52, 61, and 2 in the percentage values of identity, homology, and gap, respectively, between the deduced amino acid sequences). The *toxE* gene is predicted to encode a RibD isozyme (a deaminase/reductase activity that converts **1** into **2** in riboflavin biosynthesis) (Magalhães et al. 2008) and *B. glumae* RibD is encoded in bglu_1g08000 (homology values of 70, 82, and 0 between ToxE and RibD). Riboflavin biosynthesis is processed through **3** (Fischer and Bacher 2005) (Fig. 1A). The *tox* operon composition supports the idea that the toxoflavin biosynthetic route shares its early two steps with that of riboflavin. However, the low level of similarity (61 %) between ToxB and *B. glumae* RibA (Bglu-RibA) and the lack of a sugar moiety in the toxoflavin structure suggest that ToxB intrinsically differs from RibA and utilizes an unidentified purine derivative, instead of GTP for its substrate.

ToxA, a *S*-adenosyl-L-methionine-dependent methyltransferase, is predicted to be an *N*-methyltransferase that mediates the final step in the biosynthesis of toxoflavin and its congeners. The biochemical mechanism involved in the conversion of **2**–**4** is totally veiled, but ToxC and ToxD can be tentatively assigned as the enzymes involved in this conversion. ToxC is a WD-40 repeat domain protein, and a biochemical role of ToxD is elusive. WD-40 repeat domain proteins are widely known for their roles in protein–protein interactions (Stirnimann et al. 2010). The conversion of **2**–**4** involves the formation of an *N*–*N* bond that is found in diverse natural products; a biochemical mechanism of this bioconversion is yet enigmatic (Blair and Sperry 2013). Toxoflavin biosynthesis can be regarded as an excellent template for elucidating the *N*–*N* bond formation mechanism due to the relative simplicity of its structure and the catalyst candidates (ToxC and ToxD) at hand. Understanding the molecular mechanisms involved in toxoflavin biosynthesis can also provide a biocatalytic tool to generate derivatives of 7-azapteridine, which can be explored as herbicides (Kim et al. 2012) or new drug candidates (Nagamatsu and Yamasaki 2001; Choi et al. 2013).

Materials and methods

Strains, culture conditions, and plasmids

Burkholderia glumae BGR1 was used in this study. *Escherichia coli* DH5α and BL21 (DE3) were used for routine DNA cloning experiments and recombinant protein expression, respectively. *E. coli* S-17 [*recA pro* (RP4-2Tet::Mu Kan::Tn7)] (Simon et al. 1983) was used for intergeneric conjugation to introduce the plasmids into *B. glumae*. All of the bacterial strains were grown or maintained in LB broth or on LB agar plates at 37 °C. Liquid cultures were maintained in a shaking incubator at 250 rpm. The antibiotics and their working concentrations used in this study were rifampicin (Rif), 50 μg/mL; kanamycin (Km), 50 μg/mL; and gentamycin (Gm), 10 μg/mL. The *Burkholderia* suicide vector pGSV3 (gentamicin resistance, Gm^r) (DeShazer et al. 2001) was used for a targeted inactivation of *toxB*. Complementation plasmids were constructed in pBBR1MCS-5 (Gm^r) (Kovach et al. 1995), except that *nptII* promoter (*nptII*p)-*toxB* was prepared in pPROBE-GTkan (Gm^r) plasmid that harbors a 131 bp *nptII*p from Tn5 in its multi-cloning site (Miller et al. 2000). pBBR1MCS-5 replicates as a low-copy number plasmid, with approximately 10 copies per cell.

Preparation and GTP cyclohydrolase II activity assay for the RibA and ToxB recombinant proteins

Bglu_ribA and *toxB* were amplified from *B. glumae* total DNA by polymerase chain reaction (PCR) with the ribA-F/-R and toxB-F/-R primer pairs, respectively (Table 1). The resulting PCR products are digested with *Nde*I and *Hind*III and cloned into the same sites in pET28b. The resulting expression constructs were introduced into *E. coli* BL21 (DE3) cells. The resulting transformants were cultured in 500 mL LB medium at 37 °C until OD_{600} reached to 0.5; then, the incubation temperature was lowered to 14 °C. Next, recombinant protein synthesis was induced by the addition of isopropyl-β-D-thiogalactopyranoside to a final concentration of 1 mM and the incubation was continued overnight at 14 °C. Purification of *N*-terminal six histidine-tagged proteins was achieved with a nickel nitrilotriacetic acid agarose resin (Qiagen, the Netherlands) according to the manufacturer's protocol. The GTP cyclohydrolase II activity assay reaction buffer contained 5 mM $MgCl_2$ and 50 mM Tris–HCl, pH 8.5. For the high-performance liquid chromatography (HPLC) analysis, 1 mM GTP was incubated with either 2.3 μM RibA (A) or 1.7 μM ToxB (B) in 100 μL at 37 °C for the indicated time period and 25 μL each of the samples was applied for HPLC separation. HPLC elution was performed on a Gemini C-18 column (150 × 2 mm, particle size of 3 μm, pore size of 11 nm; Phenomenex, USA) with a ProStar system (Varian, USA). The column was eluted with isopropanol/triethylamine/85 % phosphoric acid/water (8:10:3:979, v/v, pH not adjusted) and monitored at 280 nm as previously reported (Ritz et al. 2001). For the ultraviolet–visible (UV–Vis) spectroscopic measurements, 0.1 mM GTP was incubated with either 1.0 μM RibA (A) or 1.2 μM ToxB (B) at the ambient temperature. A UV–Vis scanning spectrophotometer (Cary50, Varian) was used for the spectroscopic measurements. The spectroscopic method was also used to determine the kinetic parameters with the varying GTP concentrations. A molar absorption coefficient of 6,280/cm at 310 nm for the GTP cyclohydrolase II product (2,5-diamino-6-β-ribosylamino-4(3*H*)-pyrimidinone 5′-phosphate) was used to calculate the activity (Grill et al. 2007).

Inactivation of *toxB*

The *toxB* inactivation construct was designed to insert kanamycin resistance gene (*kan*) inside *toxB*. The primers used in this study are shown in Table 1. The *B. glumae* genomic DNA encompassing *toxB*, its 1,223 bp upstream, and 2,106 bp downstream region were amplified with the dtoxB-F/-R primer pair. The PCR product was cloned into *Xba*I and *Kpn*I sites in pBluscript II KS (Stratagene, USA), generating pKS-toxB. *kan* gene was amplified with the Kan-F/-R primer pair from pMKm2 (Um et al. 2011) and inserted into the *Bgl*II site inside *toxB* in pKS-toxB through the In-Fusion cloning method (Clontech, USA) to generate pKS-dtoxB. Then, pKS-dtoxB was used as the template for Δ*toxB*::*kan* DNA amplification with the dtoxB-pGSV3-F/dtoxB-pGSV3-R primer pair. The Δ*toxB*::*kan* fragment was cloned into the *Xba*I and *Dra*I sites in pGSV3 to generate pTBKG. We have introduced pTBKG into *B. glumae* for *toxB* inactivation but failed in getting kanamycin resistant (Km^r) and gentamicin-sensitive phenotype. All of the exconjugants displayed Km^r and Gm^r phenotype, which is indicative of the single crossover-mediated plasmid integration event. One of these single crossover exconjugants was subjected to plasmid curing procedure but it failed. A genotyping study revealed that the single crossover-mediated plasmid integration exclusively happened at the *toxB* downstream region. Thus, we modified pTBKG by extending the size of the upstream region. Additional 2,242 bp upstream region was amplified with the Up-tox-F/-R primer pair. The PCR product was cloned into pTBKG through the In-Fusion cloning method to generate pTBKG-2.2. Intergeneric conjugation method with *E. coli* S17-1 was used to introduce pTBKG-2.2 in *B. glumae*. In details, 50 μL each of overnight cultures of *E. coli* S17-1/pTBKG-2.2 and *B. glumae* was inoculated in

Table 1 Oligonucleotide primers used in this study

Primer name	Sequence (5′–3′)[a]
dtoxB-F	ATT*TCTAGA*CAAGCGTCGTGAGTTGATGT
dtoxB-R	ATT*GGTACC*GTTCGGATTGTCAGCCAACT
Kan-F	TATCGCCTGC*AGATCT*TGTGTCTCAAAATCTCTG
Kan-R	AGTCCCTGCG*AGATCT*TTAACCAATTCTGATTAG
ribA-F	ATT*CATATG*TTTTCCATGCCTTCG
ribA-R	ATT*AAGCTT*TTATTCGTTCTCGTCGAA
toxB-F	ATT*CATATG*CGCGCGTATCTCCCG
toxB-R	ATT*AAGCTT*TCATTGCATTTCTCCGTT
dtoxB-pGSV3-F	ATT*TCTAGA*CAAGCGTCGTGAGTTGATGT
dtoxB-pGSV3-R	ATT*TTTAAA*GTTCGGATTGTCAGCCAACT
Up-tox-F	GCCGCACTAG*TCTAGA*TCGATAGTCGAACTGGTGCT
Up-tox-R	ACGACGCTTG*TCTAGA*CGTCTTCATGCGAAATGCAT
toxAB-F	ATT*TCTAGA*TTTCCGGTCGAATCCTTCGA
toxAB-R	ATT*AAGCTT*AGGATCACCTGATTGTCGTA
toxABC-R	ATT*AAGCTT*TGCAGGATCGGATGGGCAAAT
toxC-F	ATT*AAGCTT*TTCGCCAACAGCGTCAACTT
toxABC-Bm-R	ATT*GGATCC*TGCAGGATCGGATGGGCAAAT
ribA-F	ATT*TCTAGA*ATGATTTCCTCGATGCGCGT
ribA-R	ATT*AAGCTT*ATACATCGATGCCTTGCCAG
ribA(141224)-R	GGCTGCGATGGGCAATCATTCGTTCTCGTCGAAGT
toxC(141224)-F	ATGATTGCCCATCGCAGCCC

[a] Engineered restriction enzyme sites are in italic and underlined

fresh 5 mL LB broth and was grown for 4 h. Cells from each culture were washed using fresh LB broth twice and resuspended in 60 μL of LB broth. The resulting cell suspensions were mixed at the varying ratios, spotted on LB agar plate, and grown overnight. The cell mixture was recovered and resuspended in 400 μL of LB broth. A 200 μL of the resulting resuspension was overlaid on LB agar plate with Km. The Km^r exconjugants were selected after 24–48 h to be tested for the sensitivity toward Gm.

B. glumae expression plasmids

The *toxB* fragment was rescued as the *Xba*I and *Hind*III fragment from the pET28a expression construct and cloned into the same sites of pLitmus28 (New England Biolabs) to generate pLitmus28-toxB. The *toxB* fragment was rescued as a *Kpn*I and *Eco*RI fragment from pLitmus28-toxB and ligated in the same sites in pPROBE_GTkan for the *toxB* expression construct of *nptII*p-*toxB*. The *toxAB* fragment including the 696 bp *toxA* upstream region (*toxA*p) and the 85 bp *toxB* downstream region was amplified with the toxAB-F/-R primer pair. The PCR product was cloned in pMD20, rescued as the *Xba*I and *Hind*III fragment, and ligated in the same sites in pBBR1MCS-5 to generate the *toxAB* expression construct. The *toxABC* fragment including the *toxA*p sequence and the 90 bp *toxC* downstream region was amplified with the toxAB-F/toxABC-R primer pair. The PCR product was cloned into pMD20, rescued as the *Xba*I and *Hind*III fragment, and ligated in the same sites in pBBR1MCS-5 to generate the *toxABC* expression construct. To generate the *toxAB-toxC* construct that has a gap between *toxAB* and *toxC*, the *toxC* fragment including the 83 bp upstream and the 90 bp downstream of *toxC* was amplified with the toxC-F/toxABC-Bm-R primer pair. The PCR product was digested with *Hind*III and *Bam*HI and cloned into the *Xba*I and *Bam*HI sites in pBBR1MCS-5 through combination with the *Xba*I and *Hind*III fragment of *toxAB*. In the resulting *toxAB-toxC* expression construct, there is 174 bp gap between *toxB* and *toxC*; the 177 bp *toxB* 3′-regions were in tandem. For the *ribA* expression construct, the *ribA* fragment including the 390 bp upstream and the 81 bp downstream of *ribA* was amplified with the ribA-F/-R primer pair. The PCR fragment was cloned into pMD20, rescued as the *Xba*I and *Hind*III fragment, and ligated in same sites in pBBR1MCS-5 to generate the *ribA* expression construct. To generate the *ribA*:*toxC* construct in which *ribA* is translationally coupled with *toxC* like the *toxBC* context, the *ribA* fragment including *ribA*p was amplified with the ribA-F/ribA(141224)-R primer pair and the *toxC* fragment including its 90-bp downstream region was amplified with the toxC(141224)-F/toxABC-R primer pair. Overlapping PCR was performed using the resulting PCR products and the ribA-F/toxABC-R primer pair. The final PCR product was cloned into pBBRMCS-5 after *Xba*I

and *Hind*III digestion. All of the expression constructs were introduced into the Δ*toxB*::*kan* mutant through the intergeneric conjugation as describe above.

Extraction and analysis of toxoflavin

LB liquid culture was routinely prepared in 50 mL culture volume in 250 mL flask. The culture was maintained for 24 h. The culture supernatant was obtained by centrifugation, and the 20 mL portion of the supernatant was subjected to organic extraction. The 20 mL supernatant extracted with 30 mL of the chloroform/methanol mixture (v/v 2:1). The chloroform layer was used for further experiments. The LB agar culture (~30 mL) was prepared by streaking method and maintained for 48 h. For the toxoflavin extraction, agar was cut into small pieces with a razorblade and chopped agar was mixed with 100 mL of chloroform to be kept overnight. The chloroform extract was then filtered through cotton. The resulting chloroform extracts were then concentrated in reduced pressure. The residue was dissolved in 1 mL of chloroform for spectroscopic analysis after proper dilution. Spectroscopic measurement of absorbance at 393 nm was previously used to determine the relative amount of toxoflavin for the samples in 80 % methanol (Chen et al. 2012). In the present spectroscopic analysis of toxoflavin, each sample was dissolved in chloroform and absorbance at 415 nm was adopted in evaluating the relative level of toxoflavin, guided by the UV–Vis absorption spectrum of the authentic toxoflavin in chloroform (see Fig. 4B). Authentic toxoflavin was kindly provided by Prof. Ingyu Hwang from Seoul National University.

Results and discussion

To determine whether ToxB is a RibA isozyme, ToxB and Bglu-RibA proteins were prepared using through *E. coli* expression (Fig. 2A, B). HPLC analysis of the reaction samples was performed using a previously described method for *E. coli* RibA characterization (Ritz et al. 2001). As shown in Fig. 2C and D, both the ToxB and Bglu-RibA recombinant proteins displayed time-dependent GTP consumption and formation of new products, which were assigned as the anomeric pair of **1**, by referring to the previous *E. coli* RibA characterization study (Ritz et al. 2001). UV–Vis absorption spectra changes in both the ToxB and Bglu-RibA reactions matched the previously published data for RibA, displaying a maximum decrease and increase of absorbance at near 255 and 300 nm, respectively (Fig. 2E, F). The substrate (GTP) and the product (**1**) of GTP cyclohydrolase II have the characteristic UV absorption at near 255 and 300 nm, respectively. Thus, the UV–Vis absorption spectra change (a decrease at 255 nm and an increase at 300 nm) was a characteristic feature of GTP cyclohydrolase II reaction and has been used to monitor GTP cyclohydrolase II activity (Spoonamore et al. 2006). These enzyme experiments confirmed that ToxB is a biochemical equivalent to Bglu-RibA, at least when considering GTP cyclohydrolase II activity. The ToxB and Bglu-RibA kinetic parameters were 2.2 ± 0.27 and 1.6 ± 0.16 for k_{cat} (min^{-1}) and 21.6 ± 10.3 and 5.6 ± 2.4 for K_m (μM), respectively. These values are comparable to the previously reported data for GTP cyclohydorlase II enzymes (Ritz et al. 2001; Spoonamore et al. 2006). To reassure the GTP cyclohydrolase II activity, formate release was also measured with a coupled assay using formate dehydrogenase and NAD^+. In this coupled assay, both ToxB and Bglu-RibA were also found to be active (data not shown). When guanine was tested for a cyclohydrolase activity, neither ToxB nor Bglu-RibA displayed the relevant activity (data not shown).

Although we substantiated that ToxB exerts a GTP cyclohydrolase II activity similar to RibA, we were unable to conclude that the early steps of toxoflavin biosynthesis were parallel to those for riboflavin biosynthesis. This is because ToxB could also have other unpredictable activities in addition to its RibA activity, making it specifically involved in toxoflavin biogenesis. To clarify this issue, we assessed whether a *toxB* is a redundant gene for *Bglu-ribA* in vivo via marker replacement gene inactivation of *toxB*. If a loss in *toxB* results in the loss of toxoflavin, then the role of *toxB* is not redundant for *Bglu-ribA*, thus implying that the biological role of *toxB* differs from that of *ribA*. Although *toxB* knockout has been previous demonstrated (Kim et al. 2004; Suzuki et al. 2004), the genetic methods used in these studies, vector-integrating gene disruption and transposon insertion, may have a suppressive effect on downstream gene transcription. Thus, we achieved *toxB* inactivation through the insertion of a kanamycin resistance gene (*kan*) lacking transcriptional terminator (Um et al. 2011) (Fig. 3A). In PCR analysis, 0.63 kb fragment, which was expected for the wild-type (WT) *toxB*, was evident in the PCR sample of the WT DNA (Fig. 3B, lane 1), and a 1.6 kb fragment, but not the 0.63 kb fragment, was amplified from the Δ*toxB*::*kan* mutants (Fig. 3B, lane 2–4). Biosynthesis of toxoflavin was abolished in a Δ*toxB*::*kan* mutant as found in spectrophotometric analysis of the organic extracts obtained from both agar and liquid cultures (Figs. 4, 5). This observation was initially interpreted as indicating that *ribA* was incapable of complementing for *toxB*, but failure to restore toxoflavin production in the Δ*toxB*::*kan* strain with *nptII*p-*toxB* suggested that the Δ*toxB*::*kan* genotype may be incorrect, requiring further investigations. We have therefore prepared several complementation plasmids and tested their abilities to restore toxoflavin production in the *toxB*::*kan*

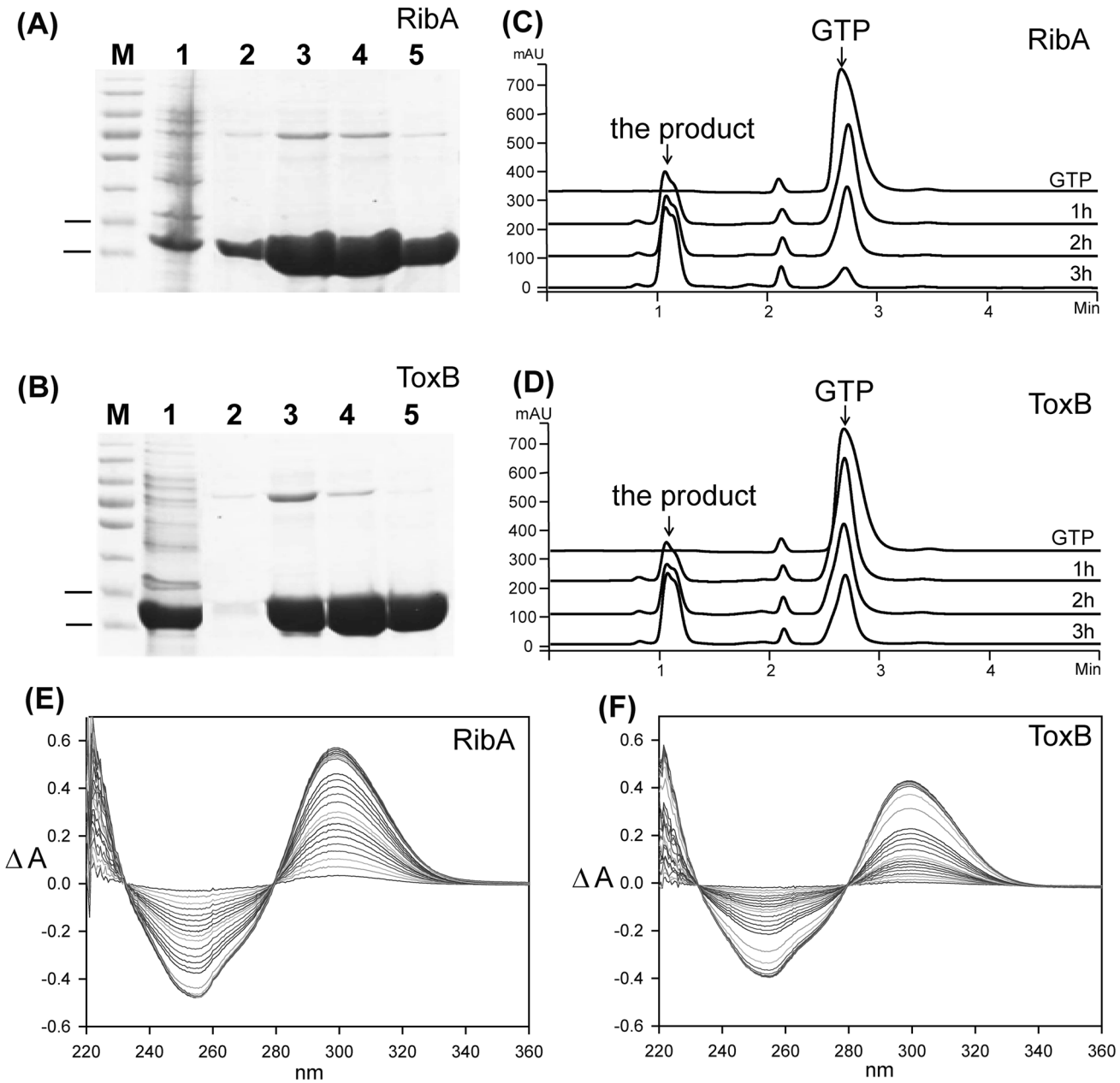

Fig. 2 Purification of the recombinant RibA (**A**) and ToxB (**B**) and their activity assay (**C**–**F**). (**A**) and (**B**) Sodium dodecyl sulfate–polyacrylamide gel electrophoresis of the six histidine-tagged recombinant RibA (**A**) and ToxB (**B**) proteins purified by a nickel affinity chromatography. The lanes indications are as follows: (M) molecular weight protein markers; (1) total soluble proteins; and (2–5) four-step imidazole elution. The 17 and 26 kDa markers are indicated with *bars* at the *left*. (**C**–**D**) HPLC traces of the RibA (**C**) and ToxB (**D**) GTP incubation products. (**E**–**F**) UV–Vis spectral changes of the RibA (**E**) and ToxB (**F**) reactions in a time-dependent manner. The zero time point was set as a blank

mutant. Because the initial trial with *nptII*p-*toxB* was unsuccessful in restoring toxoflavin production, native promoters upstream of *toxA* and *ribA* were included (coined *toxA*p and *ribA*p, respectively) in the following complementation constructs. The native *toxA*p region was previously determined by Kim et al. (2009). *Bglu-ribA* and an inosine-5-monophosphate dehydrogenase gene are divergently arranged with a 150 bp intergenic region. We intuitively adopted a 200 bp region upstream of *ribA* as *ribA*p. Using these sequences, we have prepared *toxAB*, *toxABC*, and *ribA* expression constructs. The translational coupling nature of *toxBC* (the starting codon of *toxC* overlaps with the termination codon of *toxB*, as ATGA) suggested the possibility that the co-translational nature of *toxBC* is critical to toxoflavin biosynthesis. To assess this issue, *ribA*:*toxC* (the TGA termination codon of *ribA* was

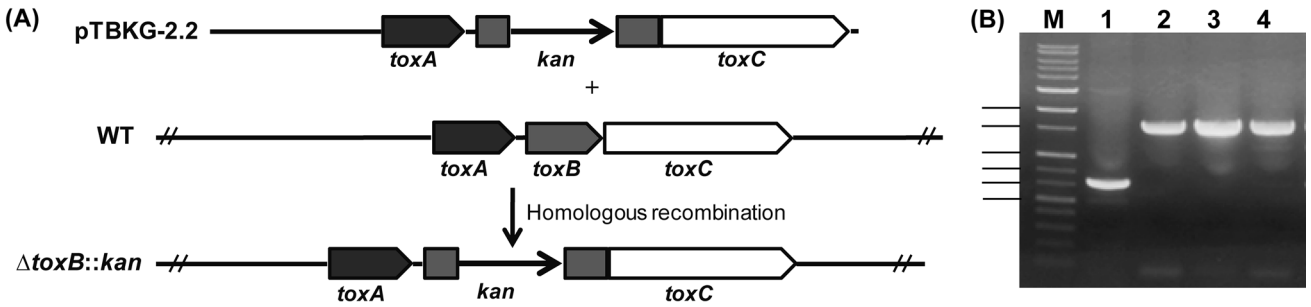

Fig. 3 The targeted inactivation of *toxB* in *B. glumae* BGR1. (**A**) Genetic map of the *toxB* inactivation construct pTBKG-2.2, *B. glumae* WT, and the Δ*toxB*::*kan* strain. (**B**) Analytical PCR of *toxB* with the toxB-F/R primer pair in WT (1) and three progeny of the Δ*toxB*::*kan* strains (2–4). M indicates the DNA marker. The 0.5, 0.65, 0.8, 1.0, 1.5, and 2.0 kb fragments are highlighted with *bars* at the *left*

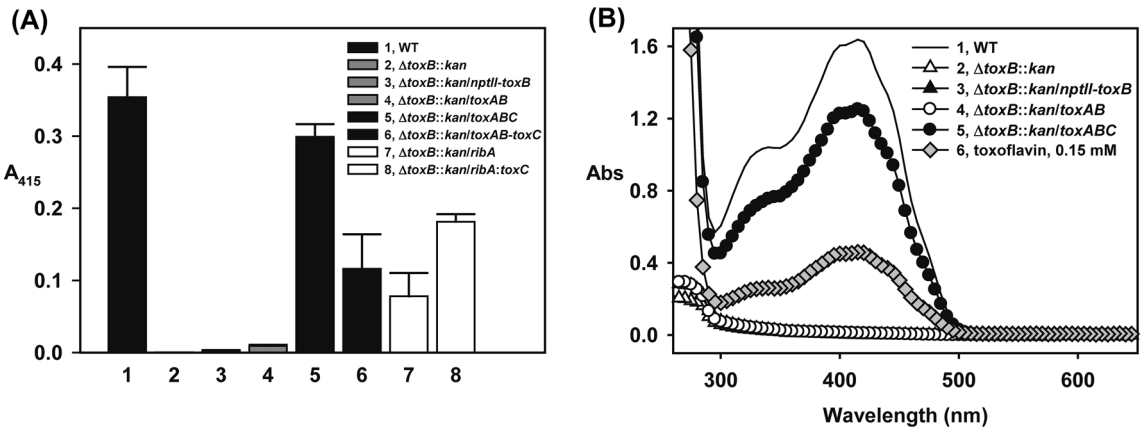

Fig. 4 Toxoflavin production of the *B. glumae* Δ*toxB*::*kan* mutant and its gene complementation derivatives in LB agar plate cultures. (**A**) Absorbance at 415 nm (A_{415}) of the extracts from WT (1), Δ*toxB*::*kan*/pBBR1MCS-5 (2), Δ*toxB*::*kan*/*nptII-toxB* (3), and Δ*toxB*::*kan*/the pBBR1MCS-5 derivatives with *toxAB* (4), *toxABC* (5), *toxAB-toxC* (6), *ribA* (7), and *ribA*:*toxC* (8). The absorbance value was calculated to be that in the original culture volume, i.e., A_{415}/mL of the culture. All of the experiments were performed in triplicate, and the standard derivations were used to draw the *error bars*. (**B**) UV–Vis absorption spectra of the extracts from WT (line), Δ*toxB*::*kan*/pBBR1MCS-5 (*unfilled triangles*), and the Δ*toxB*::*kan* transformants of *nptII-toxB* (*filled triangles*), *toxAB* (*unfilled circles*), *toxABC* (*filled circles*), and approximately 0.15 mM toxoflavin (*grey filled diamonds*)

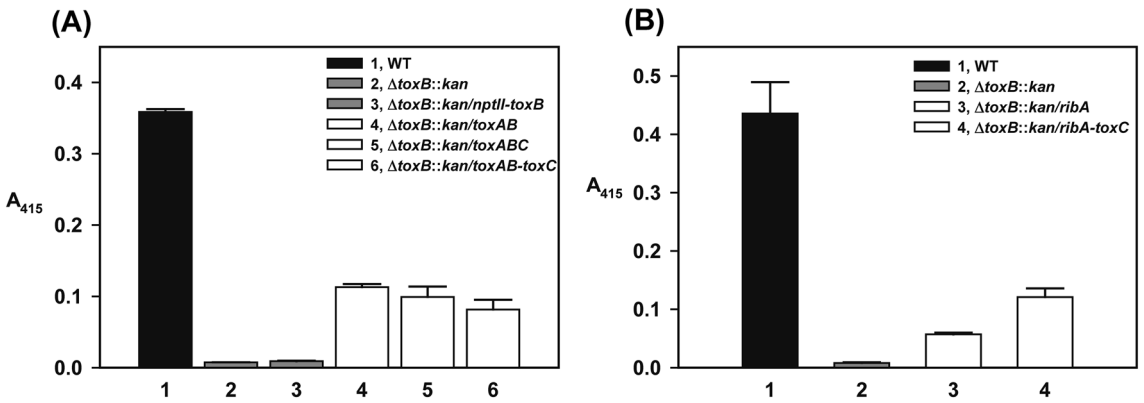

Fig. 5 Toxoflavin production of the *B. glumae* Δ*toxB*::*kan* mutant and its gene complementation derivatives in LB liquid plate culture. (**A**) A_{415} of the extracts of WT (1), Δ*toxB*::*kan*/pBBR1MCS-5 (2), Δ*toxB*::*kan*/*nptII-toxB* (3), and Δ*toxB*::*kan*/the pBBR1MCS-5 derivatives with *toxAB* (4), *toxABC* (5), and *toxAB-toxC* (6). (**B**) A_{415} of the extracts from WT (1), Δ*toxB*::*kan*/pBBR1MCS-5 (2), and the Δ*toxB*::*kan*/the pBBR1MCS-5 derivatives with *ribA* (3), and *ribA*:*toxC* (4). The absorbance value was calculated to be that in the original culture volume, i.e., A_{415}/mL of the culture. All of the experiments were performed in triplicate, and the standard derivations were used to draw the *error bars*. The experiments shown in A and B were performed separately

engineered to overlap with the ATG start codon of *toxC*, to be ATGA) and *toxAB-toxC* (artificial interval of 200 bp between *toxB* and *toxC*) were also prepared.

In LB agar cultures prepared via a streaking method, neither *nptII-toxB* nor *toxAB* restored toxoflavin production, while both *toxABC* and *toxAB-toxC* did. The toxoflavin levels in the *toxABC* complementation were significantly higher than in *toxAB-toxC* and were comparable to that of WT (Fig. 4A). UV–Vis absorption spectra of selected samples are shown in Fig. 4B. This observation indicates that a co-expression of *toxB* and *toxC* is critical for toxoflavin biosynthesis and that translation coupling fortifies the co-expression effects. Considering that ToxC is a WD repeat domain protein, association of ToxB and ToxC can be envisioned. Contrary to the case of *toxAB* expression, *ribA* alone successfully induced toxoflavin biosynthesis in the Δ*toxB*::*kan* mutant, with *ribA*:*toxC* having higher toxoflavin levels. This suggests that *ribA* with its plasmid copies (approximately 10 copies) can complement for the loss of *toxB*, even though the chromosomal copy was incapable of doing so. To check the possibility that the *ribA* 3′-UTR region negatively regulated *ribA* expression, 600 bp of the 3′-UTR region was included in another *ribA* expression plasmid. This resulting plasmid also induced toxoflavin production in the Δ*toxB*::*kan* mutant (data not shown). Thus, we concluded that the multiple copies of *ribA* enhanced RibA levels and that this unusually high level of RibA could substitute for ToxB activity in the Δ*toxB*::*kan* mutant. The transcription of *toxA*p may be tightly controlled; thus, an increase in the copy number did not result in an increase in expression level. The relatively slow growth on agar plates may be related to a tight regulation on *toxA*p expression. Toxoflavin biosynthetic genes have been very recently characterized in *Pseudomonas protegens* Pf-5 (Philmus et al. 2015). The authors found a trace amount of toxoflavin in an in-frame *toxB* deletion mutant and deduced that *ribA* complemented for the loss of *toxB*. With this observation, the authors suggest that ToxB is a RibA isozyme. However, there is no evidence that shows that *ribA* is truly responsible for toxoflavin production in the Δ*toxB* mutant. In our experiment, we confirmed this notion by introducing *ribA* into the Δ*toxB*::*kan* mutant and detecting substantial toxoflavin levels in the resulting strain. When *toxE* was inactivated in *P. protegens* Pf-5, toxoflavin was readily found, suggesting that *ribD* efficiently substituted for *toxE* in toxoflavin production (Philmus et al. 2015). It is important to note that the spectroscopic quantification may not only reflect toxoflavin but also its congeners, such as fervenulin and reumycin. However, we used the terminology *toxoflavin production* for simplicity.

In LB liquid cultures, all three of the *toxB*-containing constructs (*toxAB*, *toxABC*, and *toxAB-toxC*) partially restored toxoflavin production (Fig. 5A). The production of toxoflavin in the *toxAB* expression transformant is rather surprising because this strain failed to generate toxoflavin in the agar solid cultures (Fig. 4A). An evident difference between solid and liquid cultures is the growth rate; a liquid culture should display faster growth. We speculate that *tox* operon expression is highly induced at an idiophase of liquid culture and that co-expression of *toxB* and *toxC* is not a critical determinant for the integrity of toxoflavin biosynthetic machinery in this condition. Cellular protein synthesis dynamics or other cellular factors during growth in liquid culture may neutralize the requirement for *toxBC* co-expression. *ribA* successfully restored toxoflavin biosynthesis at the higher level with the *ribA*:*toxC* construct (Fig. 5B), which was also observed in the agar culture experiment (Fig. 4A).

Biochemical characterization, *toxB* inactivation, and the gene complementation experiments demonstrated that ToxB is a functional GTP cyclohydrolase II. This substantiated that toxoflavin biosynthesis shares the early steps with riboflavin biosynthesis, providing a platform to trace the unique biochemistry involved in toxoflavin biosynthesis. Hypothetically, 5,6-diaminouracil may not be a true intermediate; *N–N* bond formation may be coupled with a removal of the ribitol moiety from **2**. ToxD might be a novel enzyme that mediates the enigmatic *N–N* bond formation. Operon structure and translational coupling between *toxB* and *toxC* appear to control toxoflavin productivity, implying the presence of a toxoflavin biosynthetic metabolon. It was recently demonstrated that the RibA product (**1**) and RibD deaminase product are toxic to *E. coli* and *Arabidopsis thaliana* and that a directed overflow mechanism by an *N*-glycosidase (COG3236) removes these reactive metabolites (however, a COG3236 gene could not be identified in the *B. glumae* genome) (Frelin et al. 2015). Frelin et al. (2015) assert that the formation of a metabolon, a multienzyme complex achieving a high metabolic flux by channeling intermediates from one enzyme to another, is a damage control mechanism against reactive intermediates in riboflavin biosynthesis. We propose that a toxoflavin biosynthetic metabolon is constituted by a scaffolding role of ToxC.

Acknowledgments This work was supported by 2015 Research Fund of Myongji University.

References

Blair LM, Sperry J (2013) Natural products containing a nitrogen-nitrogen bond. J Nat Prod 76:794–812

Chen R, Barphagha IK, Karki HS, Ham JH (2012) Dissection of quorum-sensing genes in *Burkholderia glumae* reveals non-

canonical regulation and the new regulatory gene *tofM* for toxoflavin production. PLoS ONE 7:e52150

Choi G, Lee J, Ji JY, Woo J, Kang NS, Cho SY, Kim HR, Ha JD, Han SY (2013) Discovery of a potent small molecule SIRT1/2 inhibitor with anticancer effects. Int J Oncol 43:1205–1211

DeShazer D, Waag DM, Fritz DL, Woods DE (2001) Identification of a *Burkholderia mallei* polysaccharide gene cluster by subtractive hybridization and demonstration that the encoded capsule is an essential virulence determinant. Microb Pathogen 30:253–269

Fischer M, Bacher A (2005) Biosynthesis of flavocoenzymes. Nat Prod Rep 22:324–350

Frelin O, Huang L, Hasnain G, Jeffryes JG, Ziemak MJ, Rocca JR, Wang B, Rice J, Roje S, Yurgel SN, Gregory JF 3rd, Edison AS, Henry CS, de Crécy-Lagard V, Hanson AD (2015) A directed-overflow and damage-control *N*-glycosidase in riboflavin biosynthesis. Biochem J 466:137–145

Gräwert T, Fischer M, Bacher A (2013) Structures and reaction mechanisms of GTP cyclohydrolases. IUBMB Life 65:310–322

Grill S, Yamaguchi H, Wagner H, Zwahlen L, Kusch U, Mack M (2007) Identification and characterization of two *Streptomyces davawensis* riboflavin biosynthesis gene clusters. Arch Microbiol 188:377–387

Kim J, Kim JG, Kang Y, Jang JY, Jog GJ, Lim JY, Kim S, Suga H, Nagamatsy T, Hwang I (2004) Quorum sensing and the LysR-type transcriptional activator ToxR regulate toxoflavin biosynthesis and transport in Burkholderia glumae. Mol Microbiol 54:921–934

Kim J, Oh J, Choi O, Kang Y, Kim H, Goo E, Ma J, Nagamatsu T, Moon JS, Hwang I (2009) Biochemical evidence for ToxR and ToxJ binding to the *tox* operons of *Burkholderia glumae* and mutational analysis of ToxR. J Bacteriol 191:4870–4878

Kim MS, Kim H, Moon JS, Hwang I, Joung H, Jeon JH (2012) Toxoflavin lyase enzyme as a marker for selecting potato plant transformants. Biosci Biotechnol Biochem 76:2354–2356

Kovach ME, Elzer PH, Hill DS, Robertson GT, Farris MA, Roop RM, Peterson KM (1995) Four new derivatives of the broad-host-range cloning vector pBBR1MCS, carrying different antibiotic-resistance cassettes. Gene 166:175–176

Levenberg B, Kaczmarek DK (1966) Enzymic release of carbon atom 8 from guanosine triphosphate, an early reaction in the conversion of purines to pteridines. Biochim Biophys Acta 117:272–275

Levenberg B, Linton SN (1966) On the biosynthesis of toxoflavin, an azapteridine antibiotic produced by *Pseudomonas cocovenenans*. J Biol Chem 241:846–852

Machlowitz RA, Fisher WP, McKay BS, Tytell AA, Charney J (1954) Xanthothricin, a new antibiotic. Antibiot Chemother 4:259–261

Magalhães ML, Argyrou A, Cahill SM, Blanchard JS (2008) Kinetic and mechanistic analysis of the *Escherichia coli ribD*-encoded bifunctional deaminase-reductase involved in riboflavin biosynthesis. Biochemistry 47:6499–6507

Miller WG, Leveau JH, Lindow SE (2000) Improved *gfp* and *inaZ* broad-host-range promoter-probe vectors. Mol Plant Microbe Interact 13:1243–1250

Nagamatsu T, Yamasaki H (2001) General syntheses of 1-alkyltoxoflavin and 8-alkylfervenulin derivatives of biological significance by the regioselective alkylation of reumycin derivatives and the rates of transalkylation from 1-alkyltoxoflavins into nucleophiles. J Chem Soc Perkin Trans 1(2):130–137

Philmus B, Shaffer B, Kidarsa T, Yan Q, Raaijmakers J, Begley T, Loper J (2015) Investigations into the biosynthesis, regulation and self-resistance of toxoflavin in *Pseudomonas protegens* Pf-5. ChemBioChem 16:1782–1790

Ren J, Kotaka M, Lockyer M, Lamb HK, Hawkins AR, Stammers DK (2005) GTP cyclohydrolase II structure and mechanism. J Biol Chem 280:36912–36919

Ritz H, Schramek N, Bracher A, Herz S, Eisenreich W, Richter G, Bacher A (2001) Biosynthesis of riboflavin: studies on the mechanism of GTP cyclohydrolase II. J Biol Chem 276:22273–22277

Sato Z, Koiso Y, Iwasaki S, Matsuda L, Shirata A (1989) Toxins produced by *Pseudomonas glumae*. Ann Phytopathol Soc Jpn 55:353–356

Schramek N, Bracher A, Bacher A (2001) Biosynthesis of riboflavin. Single turnover kinetic analysis of GTP cyclohydrolase II. J Biol Chem 276:44157–44162

Simon R, Prifer U, Puhler A (1983) A broad range mobilization system for in vivo genetic engineering: transposon mutagenesis in Gram-negative bacteria. Biotechnology 1:784–791

Spoonamore JE, Dahlgran AL, Jacobsen NE, Bandarian V (2006) Evolution of new function in the GTP cyclohydrolase II proteins of *Streptomyces coelicolor*. Biochemistry 45:12144–12155

Stirnimann CU, Petsalaki E, Russell RB, Müller CW (2010) WD40 proteins propel cellular networks. Trends Biochem Sci 35:565–574

Suzuki F, Sawada H, Azegami K, Tsuchiya K (2004) Molecular characterization of the *tox* operon involved in toxoflavin biosynthesis of *Burkholderia glumae*. J Gen Plant Pathol 70:97–107

Um HY, Chung E, Lee JH, Lee SW (2011) Improved antibiotic resistance gene cassette for marker exchange mutagenesis in *Ralstonia solanacearum* and *Burkholderia* species. J Microbiol 49:305–308

Yoneyama K, Kono Y, Yamaguchi I, Horikoshi M, Hirooka T (1998) Toxoflavin is an essential factor for virulence of *Burkholderia glumae* causing rice seedling rot disease. Ann Phytopathol Soc Jpn 64:91–96